



CERN-EP-2022-171
08 August 2022

Measurements of groomed-jet substructure of charm jets tagged by D^0 mesons in proton–proton collisions at $\sqrt{s} = 13$ TeV

ALICE Collaboration*

Abstract

Understanding the role of parton mass and Casimir colour factors in the quantum chromodynamics parton shower represents an important step in characterising the emission properties of heavy quarks. Recent experimental advances in jet substructure techniques have provided the opportunity to isolate and characterise gluon emissions from heavy quarks. In this work, the first direct experimental constraint on the charm-quark splitting function is presented, obtained via the measurement of the groomed shared momentum fraction of the first splitting in charm jets, tagged by a reconstructed D^0 meson. The measurement is made in proton–proton collisions at $\sqrt{s} = 13$ TeV, in the low jet transverse-momentum interval of $15 \leq p_T^{\text{jet ch}} < 30$ GeV/ c where the emission properties are sensitive to parton mass effects. In addition, the opening angle of the first perturbative emission of the charm quark, as well as the number of perturbative emissions it undergoes, is reported. Comparisons to measurements of an inclusive-jet sample show a steeper splitting function for charm quarks compared with gluons and light quarks. Charm quarks also undergo fewer perturbative emissions in the parton shower, with a reduced probability of large-angle emissions.

arXiv:2208.04857v2 [nucl-ex] 27 Nov 2023

*See Appendix B for the list of collaboration members

In hadronic collisions, quarks and gluons (partons) with high transverse momentum (p_T) and/or large masses are produced in scattering processes involving large momentum transfers. These energetic partons lose their large initial virtuality by emitting partons in a cascade process known as a parton shower, until they eventually form hadrons. Theoretical descriptions of parton showers rely on determining the emission probability of partons, which are described by splitting functions [1, 2]. Splitting functions are universal properties of quantum chromodynamics (QCD) that describe how the energy of a parton is shared as it fragments into further partons. The splitting functions of light-flavour (up, down, and strange) quarks and gluons differ due to their different Casimir colour factors [2]. For heavy-flavour (charm and beauty with masses of $(1.27 \pm 0.02) \text{ GeV}/c^2$ and $4.18^{+0.03}_{-0.02} \text{ GeV}/c^2$, respectively [3]) quarks the splitting functions are strongly influenced by the large quark mass [4]. As a consequence, the radiation pattern of the parton shower depends on the type of initiating parton.

Experimental access to the parton shower can be gained via measurements involving jets, which are collimated bunches of hadrons resulting from the fragmentation of partons scattered in the initial stages of collisions. Jets represent a powerful tool for testing perturbative QCD, as their inner structure (substructure) reflects the properties of the underlying parton shower. Measurements of jet substructure have been performed in inclusive jets (with no flavour tagging) to constrain the splitting functions of light quarks and gluons [5–8]. However, an experimentally clean separation of gluon-initiated and quark-initiated jets has remained challenging, with measurements constraining the splitting functions comprising an admixture of the two subsets.

Recent experimental advances in techniques pertaining to the substructure of heavy-flavour jets [9, 10] have allowed for the isolation and study of gluon emissions from heavy quarks. This technique has been used to perform a first direct measurement [11] of the dead-cone effect [12] in charm-quark jets. The dead cone corresponds to an angular region along the flight direction of the emitter, with an opening proportional to the ratio of mass to energy of the emitter, within which the probability of emissions is suppressed. The significant size of this region for low-energy heavy-flavour quarks gives rise to mass-dependent effects in the parton shower. In addition to the sensitivity to these mass effects in QCD, heavy-flavour jets represent an experimentally enhanced quark-initiated jet sample, which can be further used to constrain the flavour-dependent properties of QCD emissions arising from different Casimir colour factors.

In this work, the first measurement directly constraining the charm-quark splitting function is reported. This requires access to perturbative splittings (the splitting scale is much larger than the QCD scale) of the charm quark, where the shared momentum fraction of the splittings maps onto the analytical splitting function [13–15]. Additionally, measurements of the opening angle of these emissions, as well as the number of perturbative emissions in charm jets, are reported. Measurements of these two observables have also been reported for inclusive jets [6–8, 16, 17], with the opening angle calculated at next-to-leading logarithmic accuracy [18]. The measurements reported in this work are made in the low jet transverse-momentum interval of $15 \leq p_T^{\text{jet ch}} < 30 \text{ GeV}/c$, where mass effects are expected to play a role in the fragmentation of the charm quark and the inclusive sample is mainly comprised of gluon-initiated jets.

Once jets have been identified from the sample of charged particles (reconstructed as tracks) in pp collisions, using the anti- k_T algorithm [19], track-based jet-substructure observables can be constructed from the jet constituents. To reconstruct the chain of emissions (splitting tree) inside a jet, the jet constituents can be reclustered with the Cambridge–Aachen (C/A) algorithm [20], which is well suited to jet substructure studies because it follows the angular ordering of emissions in QCD [1] by clustering the jet constituents based on their angular distance. By following a branch along the splitting tree returned by the reclustering procedure, a sequence of emissions can be studied [21].

Charm jets are identified by the presence of a reconstructed D^0 meson amongst their constituents. The full reconstruction of the $D^0 \rightarrow K^- \pi^+$ decay allows for the replacement of the D^0 decay products with the four-momentum of the D^0 meson, prior to jet clustering. This ensures that the full D^0 -meson momentum is contained within the jet cone. As the charm flavour is conserved throughout the jet evolution, the charm quark can be traced as it dynamically evolves in the showering process, by following the branch containing the D^0 meson through the splitting tree [9].

To reduce the contribution of non-perturbative effects and increase sensitivity to perturbative emissions [22], the Soft Drop grooming procedure [23] is applied, which only selects particular splittings of interest along the followed branch. To do this, each splitting along this branch is tested against the Soft Drop condition, as given by

$$z \equiv \frac{\min(p_{T,1}, p_{T,2})}{p_{T,1} + p_{T,2}} > z_{\text{cut}} \left(\frac{\Delta R_{1,2}}{R} \right)^\beta, \quad (1)$$

where $p_{T,1}$ and $p_{T,2}$ are the transverse momenta of the leading and subleading prongs of the splitting, respectively, and R is the jet resolution parameter. The grooming behaviour is determined by the parameters z_{cut} and β , which control the interplay between the shared momentum fraction, z , and the aperture angle between the prongs, $\Delta R_{1,2} \equiv \sqrt{(y_1 - y_2)^2 + (\varphi_1 - \varphi_2)^2}$, where y and φ are the rapidity and azimuth of prongs 1 and 2, respectively. In this work, values of $z_{\text{cut}} = 0.1$ and $\beta = 0$ are chosen, such that the Soft Drop condition is satisfied if the subleading prong carries at least 10% of the sum of the transverse momenta of the prongs, enriching the selection with perturbative splittings.

Two groomed substructure observables are constructed against the first splitting that satisfies the Soft Drop condition: $z_g = z$ and $R_g = \Delta R_{1,2}$, as given in Eq. 1. For the given choices of grooming parameters, the shared momentum fraction, z_g , converges to the QCD splitting function at sufficiently high jet energies [13]. As the emissions are angular ordered, the groomed emission angle R_g characterises the widest emission in the splitting tree which passes the Soft Drop condition and sets the geometrical scale of the jet. This observable is expected to be sensitive to the dead cone of the charm quark at small angles, whilst emissions from gluons, which have a larger Casimir colour factor, are expected to dominate the large-angle region [24, 25]. The number of emissions of the charm quark satisfying the Soft Drop condition, n_{SD} , is also measured by evaluating all splittings along the branch containing the D^0 meson. This strongly correlates to the number of perturbative emissions of the charm quark.

The data were collected using the ALICE apparatus at the LHC, during the years 2016, 2017, and 2018. Information about the detector configuration and performance can be found in Refs. 26, 27. The main detector systems used for this work were the central-barrel detectors, located at $|\eta| < 0.9$ within a solenoidal magnet and used for charged-particle tracking and identification. These include the Inner Tracking System, the Time Projection Chamber, and the Time-Of-Flight detector. The V0 detector, consisting of two scintillator arrays located at pseudorapidities of $2.8 < \eta < 5.1$ and $-3.7 < \eta < -1.7$, was used for the trigger and event selections. Minimum-bias events were selected by requiring a signal above a given threshold in both V0 counters. The analysed data sample consisted of about 1.7×10^9 pp collisions at a centre-of-mass energy of $\sqrt{s} = 13$ TeV, corresponding to an integrated luminosity of $\mathcal{L}_{\text{int}} = 29 \text{ nb}^{-1}$.

The D^0 mesons were reconstructed in the $D^0 p_T$ interval of $5 \leq p_T^{D^0} < 30 \text{ GeV}/c$, through the $D^0 \rightarrow K^- \pi^+$ (and charge conjugate) decay channel with a branching ratio of $(3.95 \pm 0.03)\%$ [3]. Background candidates, built from pairs of tracks not corresponding to a D^0 decay, were suppressed by applying geometrical selections on the displaced-decay-vertex topology, as well as particle identification on the decay-particle tracks [28]. The D^0 decay daughters were replaced in the event by the D^0 -meson four-momentum, which was obtained by summing the four-momenta of these decay daughters. Jet finding was then performed using the FastJet package [29], with the anti- k_T algorithm, a resolution parameter of $R = 0.4$ and the E -scheme recombination. The inputs to the jet finder consisted of tracks of charged particles with $p_T \geq 0.15 \text{ GeV}/c$ and the reconstructed D^0 -meson candidate. The full set of quality

selections applied to the tracks, including the D^0 -meson candidate decay tracks, is given in Ref. 30. The jets were required to be fully contained within the central barrel acceptance, by imposing a pseudorapidity selection of $|\eta| < 0.5$ on the jet axis. For every D^0 meson candidate in an event, jet finding was performed independently, with only the two tracks forming that particular candidate replaced with the sum of their four-momenta prior to the jet finding pass. Once jet finding had been performed, the D^0 -tagged jet constituents were reclustered using the C/A algorithm and the z_g , R_g , and n_{SD} observables were calculated for each jet. The contribution to the three observable distributions from jets tagged by background D^0 candidates that survived the selection was removed via a sideband subtraction procedure, as detailed in Refs. 30, 31. This procedure provides the true D^0 -tagged jet observable distributions in intervals of $p_T^{D^0}$.

Each of these background-subtracted distributions was scaled by the selection and reconstruction efficiency of prompt (charm-showering) D^0 -tagged jets, estimated in $p_T^{D^0}$ intervals, from Monte Carlo (MC) simulations using PYTHIA 8.243 [32–34] and GEANT 3 [35]. The efficiency-corrected distributions were summed over the full $p_T^{D^0}$ range considered for the analysis. In order to study emissions in the charm-quark shower, the contribution from non-prompt D^0 mesons (feed-down contribution), originating from the decay of beauty hadrons, was estimated using POWHEG [36] simulations with PYTHIA 6.425 [33] showering and decays implemented through the EvtGen package [37]. It was then subtracted from the measured distributions. The magnitude of this non-prompt contribution ranged from 20% to 40% in most of the z_g , R_g , and n_{SD} intervals considered in the analysis. The $p_T^{\text{jet ch}}$ distributions and each prompt D^0 -tagged jet substructure observable were simultaneously corrected for detector effects via a two-dimensional unfolding, using the iterative Bayesian unfolding algorithm with four iterations [38].

The z_g , R_g , and n_{SD} jet observables were also measured for inclusive jets. To allow for direct comparisons with the heavy-flavour results, the constraint on the Q^2 value of the parton scattering implied by the selection of D^0 mesons with $p_T^{D^0} \geq 5 \text{ GeV}/c$ was mimicked for inclusive jets, by requiring a leading track with $p_T \geq 5.33 \text{ GeV}/c$. This corresponds to the p_T of a charged pion with the same transverse mass as a D^0 meson with $p_T^{D^0} = 5 \text{ GeV}/c$. In addition, during the grooming procedure, the hardest branch of the splitting tree was followed. In the heavy-flavour sample, following the hardest branch was found to coincide with following the branch containing the D^0 , in over 99% of cases. The inclusive-jet distributions were then corrected for detector effects via the same unfolding procedure as in the D^0 -tagged jet case.

Systematic uncertainties related to the reconstruction and identification of prompt D^0 -tagged jets were studied. The stability of the selections applied to the D^0 -meson candidates were estimated by loosening and tightening the topological and particle identification criteria used to identify the D^0 decays. The uncertainty pertaining to the signal extraction procedure was estimated by changing the fitting parameters on the invariant-mass fits, as well as the widths of the signal and sideband regions used for the sideband subtraction procedure. The uncertainty on the D^0 feed-down estimation was obtained by varying the renormalisation and factorisation scales, as well as the mass of the beauty quark, in the POWHEG simulations [39]. The uncertainty on the jet energy resolution was estimated by artificially reducing the tracking efficiency used to generate the unfolding response matrix by 4%, in line with the tracking efficiency uncertainty of the ALICE detector. Finally, the uncertainty associated with the unfolding procedure was obtained by varying the number of iterations, the choice of prior, and the ranges of the response matrix. Additionally, variations of the fragmentation properties of the MC simulation used to construct the response matrix were also included. These were obtained by reweighting the response matrix based on the value of the jet-angularity observable [40] ($\kappa = 1$ and $\beta = 1$) calculated for each entry, as this observable is sensitive to the transverse momentum and angular distribution of all hadrons in the jet. The weights were devised such that the reweighting procedure transformed the angularity distribution at generator level of the D^0 -tagged jets in the response matrix, to match that of a simulated inclusive-jet distribution.

The dominant contributions in most of the intervals resulted from variations of the topological selections, signal extraction, and feed-down subtraction. For the feed-down subtraction uncertainty, the maximum

negative and the maximum positive deviations were taken, respectively. For each of the other variation categories, the root mean square of deviations from the central values was calculated and assigned as a systematic uncertainty, which was then symmetrised around the central value. The uncertainties from all categories were then added in quadrature to obtain the full systematic uncertainty. The total systematic uncertainties range from 7% to 77%, from 9% to 12%, and from 5% to 59% for the D^0 -tagged jet z_g , R_g , and n_{SD} distributions, respectively.

The systematic uncertainties for the inclusive-jet distributions were estimated by performing variations of the tracking efficiency and unfolding, in the same way as in the D^0 -tagged jet case. In addition, the p_T selection on the leading track of the jet was also varied in line with the track p_T resolution of the D^0 -decay tracks. The total systematic uncertainties range from 1.4% to 4.3%, from 2.2% to 5.7%, and from 3.3% to 8.1% for the inclusive-jet z_g , R_g , and n_{SD} distributions, respectively.

The first measurement mapping onto the charm-quark splitting function is reported via the z_g distribution in Fig. 1, for charm jets tagged by a prompt D^0 meson. The R_g and n_{SD} distributions are shown in the left and right panels of Fig. 2, respectively. These distributions are fully corrected for detector effects and are reported in the jet transverse-momentum interval of $15 \leq p_T^{\text{jet ch}} < 30 \text{ GeV}/c$. Each charm-tagged jet measurement is accompanied by a measurement of an inclusive-jet sample in the same kinematic interval, also fully corrected for detector effects. Both the charm-tagged jet and inclusive-jet distributions are normalised to the total number of jets in each respective category, irrespective of whether they had a splitting passing the Soft Drop condition or not. In this way, the distributions are sensitive to the proportion of jets that do not have any splittings passing the Soft Drop condition, denoted as the SD-untagged fraction. These fractions are 22% and 2.8%, in the charm-tagged jet and inclusive jet samples, respectively. Both samples are compared to PYTHIA 8 simulations and also to POWHEG + PYTHIA 6 simulations for the charm-tagged jets. The ratios of predicted distributions from parton-shower models to the measured distributions are also shown in the bottom panels of Figs. 1 and 2. A comparison of the measured z_g distribution to analytical calculations performed in the soft-collinear effective theory (SCET) framework [41, 42] can be found in Appendix A.

The z_g distributions show that charm-tagged jets have significantly fewer symmetric splittings (large z_g values), compared with inclusive jets. This is consistent with theoretical predictions [10] of the role of mass effects in the QCD splitting function. The R_g distribution for charm quarks shows a reduction at large-angles compared with inclusive jets. This can be due to the differences between quark and gluon fragmentation, with the gluon-dominated inclusive sample expected to feature larger-angle perturbative emissions. The charm and inclusive-jet distributions are consistent at small R_g . This could be due to an interplay between the dead-cone effect, which suppresses small-angle emissions from the charm quark, and the more abundant emissions from quarks compared with gluons at small angles, as gluons lose more of their initial virtuality through larger-angle emissions. The n_{SD} distribution shows a significant shift to smaller values for the charm-tagged jets ($\langle n_{SD} \rangle = 1.34 \pm 0.08 \text{ (stat.)} \pm 0.07 \text{ (syst.)}$) compared with inclusive jets ($\langle n_{SD} \rangle = 2.31 \pm 0.01 \text{ (stat.)} \pm 0.02 \text{ (syst.)}$). This indicates that, compared with light and massless partons, charm quarks on average emit fewer gluons with a large enough p_T to pass the Soft Drop condition in the showering process. This is consistent with the expectation from the presence of a dead cone for charm quarks, which results in a harder fragmentation of charm quarks compared with light quarks and gluons.

For all three observables, both the PYTHIA 8 and POWHEG + PYTHIA 6 predictions for charm-quark jets describe the measurements within uncertainties. For the more precise inclusive measurements, PYTHIA 8 exhibits some tension, particularly for the n_{SD} observable. This may be partially due to the poorly constrained quark and gluon fractions in the inclusive sample at low $p_T^{\text{jet ch}}$. In contrast, as the D^0 -tagged jets represent a quark-enriched sample, the comparison of the shower generators to data is less reliant on this fraction and can instead be used to more accurately study the mechanisms underpinning the shower properties.

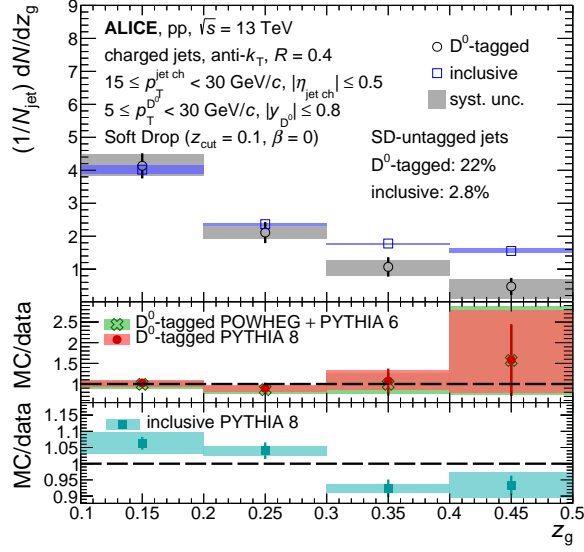


Figure 1: The z_g distribution of prompt D^0 -tagged jets compared to that of inclusive jets for $15 \leq p_T^{\text{jet ch}} < 30 \text{ GeV}/c$ in pp collisions at $\sqrt{s} = 13 \text{ TeV}$, normalised to the total number of jets. Model/data ratios are shown in the bottom panels for PYTHIA 8 [32–34] and POWHEG [36] + PYTHIA 6 [33] simulations.

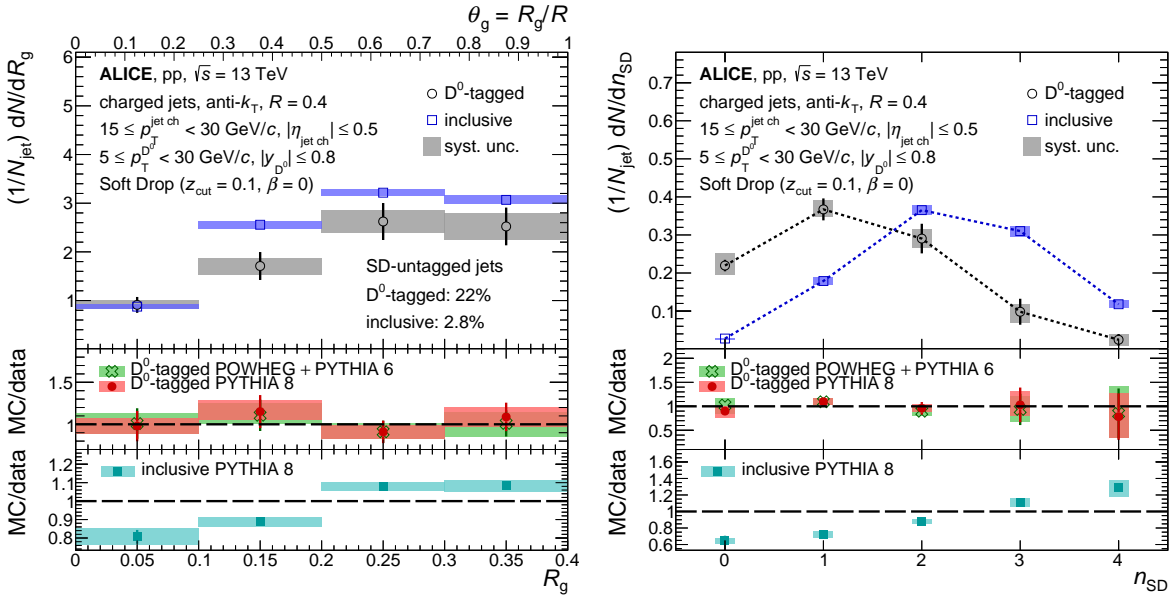


Figure 2: The R_g (left) and n_{SD} (right) distributions of prompt D^0 -tagged jets compared to those of inclusive jets for $15 \leq p_T^{\text{jet ch}} < 30 \text{ GeV}/c$ in pp collisions at $\sqrt{s} = 13 \text{ TeV}$. Model/data ratios are shown in the bottom panels for PYTHIA 8 [32–34] and POWHEG [36] + PYTHIA 6 [33] simulations.

The measurement of the groomed shared momentum fraction, z_g , of charm-tagged jets, reported in this Letter, represents the first direct experimental constraint of the splitting function of heavy-flavour quarks. The z_g distribution appears steeper than that of light quarks and gluons, with a suppressed probability of symmetric emissions. Measurements of the number of splittings passing the Soft Drop condition as well as the emission angle of the first of these splittings, show that heavy-flavour quarks on average have fewer perturbative emissions compared with light quarks and gluons, with a lower probability of these emissions occurring at large angles. These different characteristics for heavy-quark emissions, compared with light quarks and gluons, constrain the roles of quark mass and Casimir colour factors in the parton shower, which are different between the two samples. The upgraded ALICE detector in the LHC Run 3 will extend this measurement to jets tagged with a fully reconstructed beauty meson [43]. Direct comparison of the two quark-enriched samples of charm-tagged and beauty-tagged jets will enable the isolation of mass effects from the effects due to Casimir colour factors. The larger projected integrated luminosity in Run 3 will also allow us to extend the charm-tagged to inclusive jet comparisons to higher $p_T^{\text{jet ch}}$, where mass effects become negligible and the remaining impact of the Casimir colour factors can be cleanly studied.

Acknowledgements

The ALICE Collaboration would like to thank all its engineers and technicians for their invaluable contributions to the construction of the experiment and the CERN accelerator teams for the outstanding performance of the LHC complex. The ALICE Collaboration gratefully acknowledges the resources and support provided by all Grid centres and the Worldwide LHC Computing Grid (WLCG) collaboration. The ALICE Collaboration acknowledges the following funding agencies for their support in building and running the ALICE detector: A. I. Alikhanyan National Science Laboratory (Yerevan Physics Institute) Foundation (ANSL), State Committee of Science and World Federation of Scientists (WFS), Armenia; Austrian Academy of Sciences, Austrian Science Fund (FWF): [M 2467-N36] and Nationalstiftung für Forschung, Technologie und Entwicklung, Austria; Ministry of Communications and High Technologies, National Nuclear Research Center, Azerbaijan; Conselho Nacional de Desenvolvimento Científico e Tecnológico (CNPq), Financiadora de Estudos e Projetos (Finep), Fundação de Amparo à Pesquisa do Estado de São Paulo (FAPESP) and Universidade Federal do Rio Grande do Sul (UFRGS), Brazil; Bulgarian Ministry of Education and Science, within the National Roadmap for Research Infrastructures 2020-2027 (object CERN), Bulgaria; Ministry of Education of China (MOEC), Ministry of Science & Technology of China (MSTC) and National Natural Science Foundation of China (NSFC), China; Ministry of Science and Education and Croatian Science Foundation, Croatia; Centro de Aplicaciones Tecnológicas y Desarrollo Nuclear (CEADEN), Cubaenergía, Cuba; Ministry of Education, Youth and Sports of the Czech Republic, Czech Republic; The Danish Council for Independent Research | Natural Sciences, the VILLUM FONDEN and Danish National Research Foundation (DNRF), Denmark; Helsinki Institute of Physics (HIP), Finland; Commissariat à l’Energie Atomique (CEA) and Institut National de Physique Nucléaire et de Physique des Particules (IN2P3) and Centre National de la Recherche Scientifique (CNRS), France; Bundesministerium für Bildung und Forschung (BMBF) and GSI Helmholtzzentrum für Schwerionenforschung GmbH, Germany; General Secretariat for Research and Technology, Ministry of Education, Research and Religions, Greece; National Research, Development and Innovation Office, Hungary; Department of Atomic Energy Government of India (DAE), Department of Science and Technology, Government of India (DST), University Grants Commission, Government of India (UGC) and Council of Scientific and Industrial Research (CSIR), India; National Research and Innovation Agency - BRIN, Indonesia; Istituto Nazionale di Fisica Nucleare (INFN), Italy; Japanese Ministry of Education, Culture, Sports, Science and Technology (MEXT) and Japan Society for the Promotion of Science (JSPS) KAKENHI, Japan; Consejo Nacional de Ciencia (CONACYT) y Tecnología, through Fondo de Cooperación Internacional en Ciencia y Tecnología (FONCICYT) and Dirección General de Asuntos del Personal Académico (DGAPA), Mexico; Nederlandse Organisatie voor Wetenschappelijk

Onderzoek (NWO), Netherlands; The Research Council of Norway, Norway; Commission on Science and Technology for Sustainable Development in the South (COMSATS), Pakistan; Pontificia Universidad Católica del Perú, Peru; Ministry of Education and Science, National Science Centre and WUT ID-UB, Poland; Korea Institute of Science and Technology Information and National Research Foundation of Korea (NRF), Republic of Korea; Ministry of Education and Scientific Research, Institute of Atomic Physics, Ministry of Research and Innovation and Institute of Atomic Physics and University Politehnica of Bucharest, Romania; Ministry of Education, Science, Research and Sport of the Slovak Republic, Slovakia; National Research Foundation of South Africa, South Africa; Swedish Research Council (VR) and Knut & Alice Wallenberg Foundation (KAW), Sweden; European Organization for Nuclear Research, Switzerland; Suranaree University of Technology (SUT), National Science and Technology Development Agency (NSTDA), Thailand Science Research and Innovation (TSRI) and National Science, Research and Innovation Fund (NSRF), Thailand; Turkish Energy, Nuclear and Mineral Research Agency (TENMAK), Turkey; National Academy of Sciences of Ukraine, Ukraine; Science and Technology Facilities Council (STFC), United Kingdom; National Science Foundation of the United States of America (NSF) and United States Department of Energy, Office of Nuclear Physics (DOE NP), United States of America. In addition, individual groups or members have received support from: Marie Skłodowska Curie, European Research Council, Strong 2020 - Horizon 2020 (grant nos. 950692, 824093, 896850), European Union; Academy of Finland (Center of Excellence in Quark Matter) (grant nos. 346327, 346328), Finland; Programa de Apoyos para la Superación del Personal Académico, UNAM, Mexico.

References

- [1] Y. L. Dokshitzer, V. A. Khoze, A. H. Mueller, and S. I. Troian, *Basics of perturbative QCD*. Ed. Frontieres, 1991.
- [2] G. Altarelli and G. Parisi, “Asymptotic freedom in parton language”, *Nuclear Physics B* **126** (1977) 298–318.
- [3] **Particle Data Group** Collaboration, P. A. Zyla *et al.*, “Review of Particle Physics”, *PTEP* **2020** (2020) 083C01. And 2021 update.
- [4] E. G. de Oliveira, A. D. Martin, M. G. Ryskin, and A. G. Shuvaev, “Treatment of heavy quarks in QCD”, *Eur. Phys. J. C* **73** (2013) 2616, arXiv:1307.3508 [hep-ph].
- [5] **CMS** Collaboration, A. M. Sirunyan *et al.*, “Measurement of the Splitting Function in pp and Pb–Pb Collisions at $\sqrt{s_{NN}} = 5.02$ TeV”, *Phys. Rev. Lett.* **120** (2018) 142302, arXiv:1708.09429 [nucl-ex].
- [6] **ALICE** Collaboration, S. Acharya *et al.*, “Measurement of the groomed jet radius and momentum splitting fraction in pp and Pb–Pb collisions at $\sqrt{s_{NN}} = 5.02$ TeV”, *Phys. Rev. Lett.* **128** (2022) 102001, arXiv:2107.12984 [nucl-ex].
- [7] **ATLAS** Collaboration, G. Aad *et al.*, “Measurement of soft-drop jet observables in pp collisions with the ATLAS detector at $\sqrt{s} = 13$ TeV”, *Phys. Rev. D* **101** (2020) 052007, arXiv:1912.09837 [hep-ex].
- [8] **STAR** Collaboration, J. Adam *et al.*, “Measurement of groomed jet substructure observables in p+p collisions at $\sqrt{s} = 200$ GeV with STAR”, *Phys. Lett. B* **811** (2020) 135846, arXiv:2003.02114 [hep-ex].
- [9] L. Cunqueiro and M. Płoskoń, “Searching for the dead cone effects with iterative declustering of heavy-flavor jets”, *Phys. Rev. D* **99** (2019) 074027, arXiv:1812.00102 [hep-ph].

- [10] P. Ilten, N. L. Rodd, J. Thaler, and M. Williams, “Disentangling heavy flavor at colliders”, *Phys. Rev. D* **96** (2017) 054019, arXiv:1702.02947 [hep-ph].
- [11] ALICE Collaboration, S. Acharya *et al.*, “Direct observation of the dead-cone effect in quantum chromodynamics”, *Nature* **605** (2022) 440–446, arXiv:2106.05713 [nucl-ex]. [Erratum: *Nature* 607, E22 (2022)].
- [12] Y. L. Dokshitzer, V. A. Khoze, and S. I. Troian, “On specific QCD properties of heavy quark fragmentation (‘dead cone’)”, *J. Phys. G* **17** (1991) 1602–1604.
- [13] A. Larkoski, S. Marzani, J. Thaler, A. Tripathy, and W. Xue, “Exposing the QCD Splitting Function with CMS Open Data”, *Phys. Rev. Lett.* **119** (2017) 132003, arXiv:1704.05066 [hep-ph].
- [14] A. J. Larkoski, S. Marzani, and J. Thaler, “Sudakov safety in perturbative QCD”, *Phys. Rev. D* **91** (2015) 111501, arXiv:1502.01719 [hep-ph].
- [15] P. Cal, K. Lee, F. Ringer, and W. J. Waalewijn, “The soft drop momentum sharing fraction z_g beyond leading-logarithmic accuracy”, *Phys. Lett. B* **833** (2022) 137390, arXiv:2106.04589 [hep-ph].
- [16] ALICE Collaboration, S. Acharya *et al.*, “Exploration of jet substructure using iterative declustering in pp and Pb–Pb collisions at LHC energies”, *Phys. Lett. B* **802** (2020) 135227, arXiv:1905.02512 [nucl-ex].
- [17] ALICE Collaboration, S. Acharya *et al.*, “Measurements of the groomed jet radius and momentum splitting fraction with the soft drop and dynamical grooming algorithms in pp collisions at $\sqrt{s} = 5.02$ TeV”, *JHEP* **05** (2023) 244, arXiv:2204.10246 [nucl-ex].
- [18] Z.-B. Kang, K. Lee, X. Liu, D. Neill, and F. Ringer, “The soft drop groomed jet radius at NLL”, *JHEP* **02** (2020) 054, arXiv:1908.01783 [hep-ph].
- [19] M. Cacciari, G. P. Salam, and G. Soyez, “The anti- k_t jet clustering algorithm”, *JHEP* **04** (2008) 063, arXiv:0802.1189 [hep-ph].
- [20] Y. L. Dokshitzer, G. D. Leder, S. Moretti, and B. R. Webber, “Better jet clustering algorithms”, *JHEP* **08** (1997) 001, arXiv:hep-ph/9707323.
- [21] F. A. Dreyer, G. P. Salam, and G. Soyez, “The Lund Jet Plane”, *JHEP* **12** (2018) 064, arXiv:1807.04758 [hep-ph].
- [22] ALICE Collaboration, S. Acharya *et al.*, “Measurements of the groomed and ungroomed jet angularities in pp collisions at $\sqrt{s} = 5.02$ TeV”, *JHEP* **05** (2022) 061, arXiv:2107.11303 [nucl-ex].
- [23] A. J. Larkoski, S. Marzani, G. Soyez, and J. Thaler, “Soft drop”, *JHEP* **05** (2014) 146, arXiv:1402.2657 [hep-ph].
- [24] OPAL Collaboration, P. D. Acton *et al.*, “A Study of differences between quark and gluon jets using vertex tagging of quark jets”, *Z. Phys. C* **58** (1993) 387–404.
- [25] CMS Collaboration, A. Tumasyan *et al.*, “Study of quark and gluon jet substructure in Z+jet and dijet events from pp collisions”, *JHEP* **01** (2022) 188, arXiv:2109.03340 [hep-ex].
- [26] ALICE Collaboration, K. Aamodt *et al.*, “The ALICE experiment at the CERN LHC”, *JINST* **3** (2008) S08002.

- [27] ALICE Collaboration, B. Abelev *et al.*, “Performance of the ALICE Experiment at the CERN LHC”, *Int. J. Mod. Phys. A* **29** (2014) 1430044, arXiv:1402.4476 [nucl-ex].
- [28] ALICE Collaboration, S. Acharya *et al.*, “Measurement of the production of charm jets tagged with D^0 mesons in pp collisions at $\sqrt{s} = 7$ TeV”, *JHEP* **08** (2019) 133, arXiv:1905.02510 [nucl-ex].
- [29] M. Cacciari, G. P. Salam, and G. Soyez, “FastJet user manual”, *Eur. Phys. J. C* **72** (2012) 1896, arXiv:1111.6097 [hep-ph].
- [30] ALICE Collaboration, S. Acharya *et al.*, “Measurement of the production of charm jets tagged with D^0 mesons in pp collisions at $\sqrt{s} = 5.02$ and 13 TeV”, *JHEP* **06** (2023) 133, arXiv:2204.10167 [nucl-ex].
- [31] ALICE Collaboration, S. Acharya *et al.*, “Groomed jet substructure measurements of charm jets tagged with D^0 mesons in pp collisions at $\sqrt{s} = 13$ TeV”, 2020. <https://cds.cern.ch/record/2719005>. ALICE-PUBLIC-2020-002.
- [32] P. Skands, S. Carrazza, and J. Rojo, “Tuning PYTHIA 8.1: the Monash 2013 tune”, *Eur. Phys. J. C* **74** (2014) 3024, arXiv:1404.5630 [hep-ph].
- [33] T. Sjöstrand, S. Mrenna, and P. Z. Skands, “PYTHIA 6.4 physics and manual”, *JHEP* **05** (2006) 026, arXiv:hep-ph/0603175.
- [34] T. Sjöstrand, S. Ask, J. R. Christiansen, R. Corke, N. Desai, P. Ilten, S. Mrenna, S. Prestel, C. O. Rasmussen, and P. Z. Skands, “An introduction to PYTHIA 8.2”, *Comput. Phys. Commun.* **191** (2015) 159–177, arXiv:1410.3012 [hep-ph].
- [35] R. Brun, F. Bruyant, M. Maire, A. C. McPherson, and P. Zancarini, *GEANT 3 : user’s guide Geant 3.10, Geant 3.11; rev. version*. CERN, Geneva, 1987. <https://cds.cern.ch/record/1119728>.
- [36] S. Alioli, P. Nason, C. Oleari, and E. Re, “A general framework for implementing NLO calculations in shower Monte Carlo programs: the POWHEG BOX”, *JHEP* **06** (2010) 043, arXiv:1002.2581 [hep-ph].
- [37] D. J. Lange, “The EvtGen particle decay simulation package”, *Nucl. Instrum. Meth. A* **462** (2001) 152–155.
- [38] G. D’Agostini, “A multidimensional unfolding method based on Bayes’ theorem”, *Nucl. Instrum. Meth. A* **362** (1995) 487–498.
- [39] M. Cacciari, P. Nason, and R. Vogt, “QCD predictions for charm and bottom production at RHIC”, *Phys. Rev. Lett.* **95** (2005) 122001, arXiv:hep-ph/0502203.
- [40] A. J. Larkoski, J. Thaler, and W. J. Waalewijn, “Gaining (Mutual) Information about Quark/Gluon Discrimination”, *JHEP* **11** (2014) 129, arXiv:1408.3122 [hep-ph].
- [41] H. T. Li and I. Vitev, “Inverting the mass hierarchy of jet quenching effects with prompt b-jet substructure”, *Phys. Lett. B* **793** (2019) 259–264, arXiv:1801.00008 [hep-ph].
- [42] H. T. Li, Z. L. Liu, and I. Vitev, “Heavy flavor jet production and substructure in electron–nucleus collisions”, *Phys. Lett. B* **827** (2022) 137007, arXiv:2108.07809 [hep-ph].
- [43] ALICE Collaboration, S. Acharya *et al.*, “Future high-energy pp programme with ALICE”,. <https://cds.cern.ch/record/2724925>. ALICE-PUBLIC-2020-005.

A Supplementary material

The measured z_g distribution is also compared to analytical calculations performed in the soft-collinear effective theory (SCET) framework with resummation to modified leading-logarithmic accuracy (MLL) [41, 42], presented in Fig. A.1, which are consistent with the data. The calculations do not include hadronisation effects and are performed utilising a leading-order evaluation of the charm cross section, which experimentally corresponds to jets with both charged and neutral information. It is expected that the low- z_g region of the calculations are affected by non-perturbative effects. For comparison with the SCET predictions, the measurement is normalised to the number of jets passing the Soft Drop condition in each sample, as the calculations are provided for $z_g \geq 0.1$ and do not include an untagged fraction.

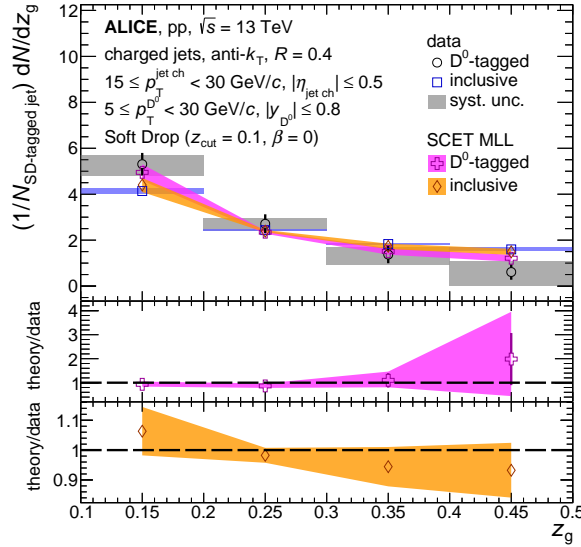


Figure A.1: The z_g distribution of prompt D^0 -tagged jets compared to that of inclusive jets for $15 \leq p_T^{\text{jet}^{\text{ch}}} < 30 \text{ GeV}/c$ in pp collisions at $\sqrt{s} = 13 \text{ TeV}$, normalised to the number of jets passing the Soft Drop condition. Model/data ratios are shown in the bottom panels for soft-collinear effective theory calculations [41, 42].

Comparisons of distributions of D^0 -tagged jets, quark-initiated jets and gluon-initiated jets, obtained with PYTHIA 8 simulations, are shown in Figs. A.2, A.3 and A.4 for the z_g , R_g and n_{SD} observables, respectively. The distributions are all normalised to the total number of jets in the kinematic range, regardless of whether they had a splitting which successfully passed the Soft Drop condition. Quark (gluon)-initiated jets are tagged by requiring an outgoing quark (gluon) from the initial hard scatter to be within $\Delta R < 0.4$ of the jet axis. Differences between the quark-initiated jet distributions and the gluon-initiated jet distributions highlight the role of Casimir colour effects in the observables, whilst differences between the quark-initiated jet distributions and the D^0 -tagged jet distributions are sensitive to mass effects. We observe that the z_g observable is not very sensitive to the different Casimir colour factors of quarks and gluons, but shows a heightened sensitivity to mass effects. The R_g distribution on the other hand is sensitive to both effects, with the larger Casimir colour factor of gluons compared to quarks resulting in broader opening angles for gluon-initiated jets. The large mass of the charm quark also results in fewer small-angle emissions, compared to the quark-initiated jet sample, as expected from the presence of a large dead-cone region around the charm quark within which emissions are suppressed. The n_{SD} distribution shows sensitivity to both Casimir and mass effects, with the impact of the latter being much more significant in this kinematic range. However, it is worth noting that flavour of emissions in the quark-tagged and gluon-tagged jets is only well defined for the first emission, whereas in the case of the D^0 -tagged jets the flavour is controlled all the way through the shower.

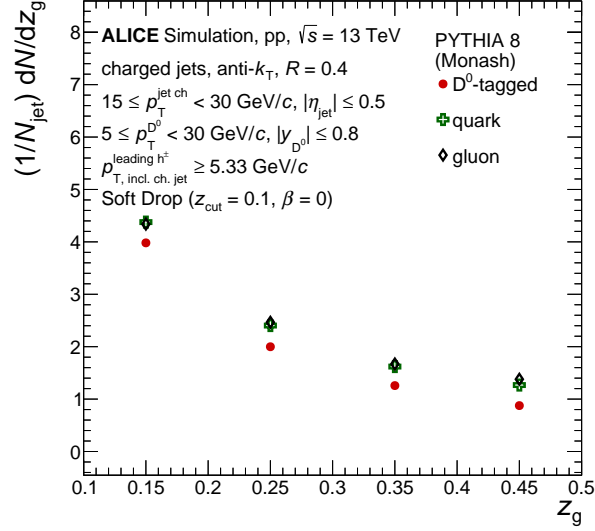


Figure A.2: PYTHIA 8 z_g distributions of prompt D^0 -tagged jets, quark-initiated and gluon-initiated jets are compared, for $15 \leq p_T^{\text{jet ch}} < 30$ GeV/c in pp collisions at $\sqrt{s} = 13$ TeV.

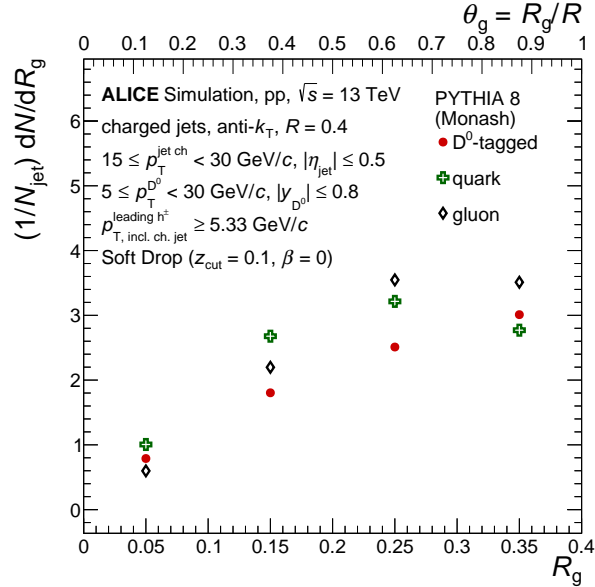


Figure A.3: PYTHIA 8 R_g distributions of prompt D^0 -tagged jets, quark-initiated and gluon-initiated jets are compared, for $15 \leq p_T^{\text{jet ch}} < 30$ GeV/c in pp collisions at $\sqrt{s} = 13$ TeV.

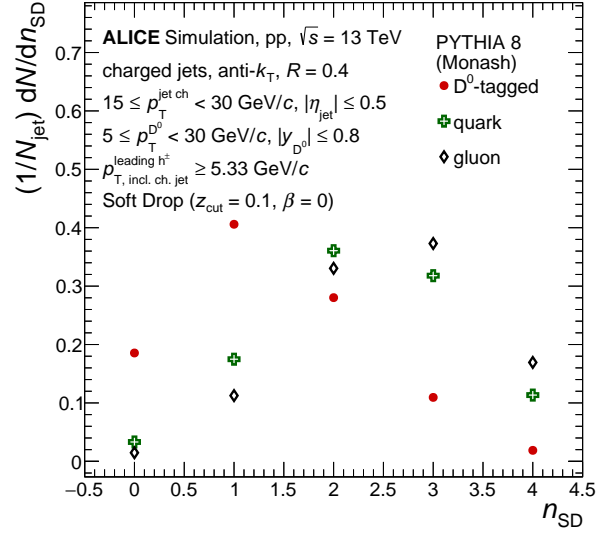


Figure A.4: PYTHIA 8 n_{SD} distributions of prompt D^0 -tagged jets, quark-initiated and gluon-initiated jets are compared, for $15 \leq p_T^{\text{jet ch}} < 30$ GeV/c in pp collisions at $\sqrt{s} = 13$ TeV.

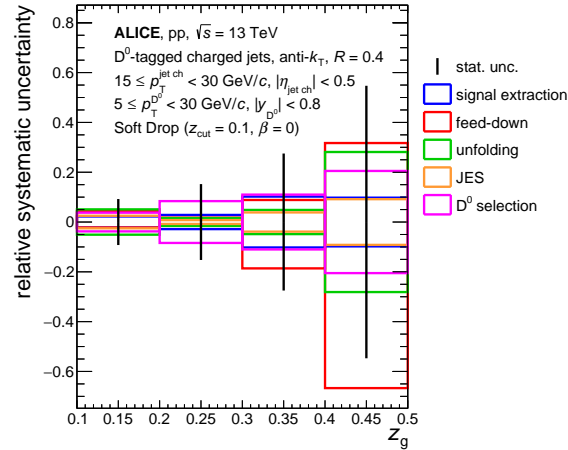


Figure A.5: The systematic uncertainties of the measured z_g distribution of prompt D^0 -tagged jets for each uncertainty category, relative to the central value of the measurement in each interval, are presented. The statistical uncertainty relative to the central value is also shown.

The systematic uncertainties of the measured z_g , R_g and n_{SD} distributions of prompt D^0 -tagged jets are presented in Figs. A.5 and A.6 for each individual uncertainty category considered (signal extraction, feed-down subtraction, unfolding, jet energy scale (JES), D^0 selection). The results are shown relative to the central values of the measured distributions in each interval. The statistical uncertainty relative to the central value is also shown for comparison.

The systematic uncertainties of the measured z_g , R_g and n_{SD} distributions of inclusive jets are presented in Figs. A.7 and A.8 for each individual uncertainty category considered (unfolding, JES and p_T selection on the leading track). The results are shown relative to the central values of the measured distributions in each interval. The statistical uncertainty relative to the central value is also shown for comparison.

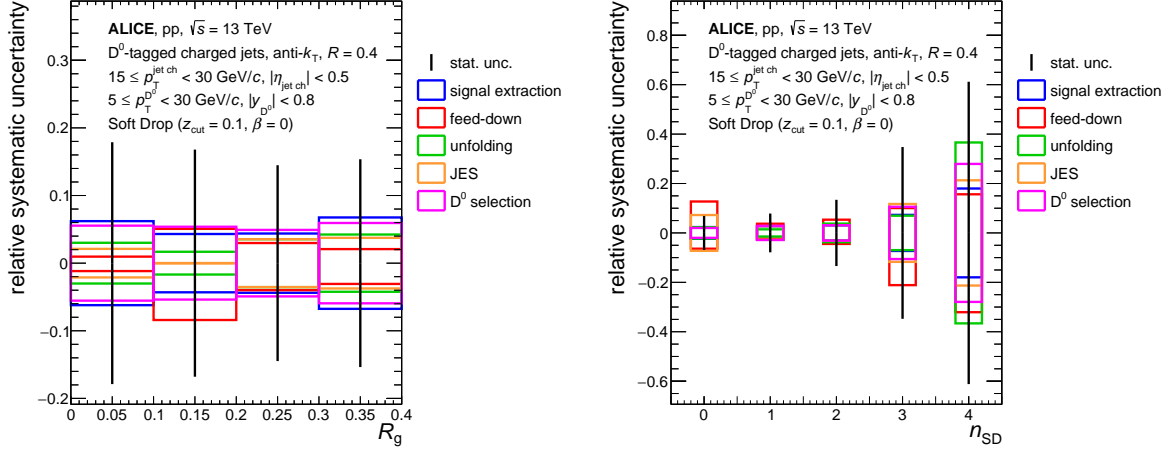


Figure A.6: The systematic uncertainties of the measured R_g (left) and n_{SD} (right) distributions of prompt D^0 -tagged jets for each uncertainty category, relative to the central value of the measurement in each interval, are presented. The statistical uncertainty relative to the central value is also shown.

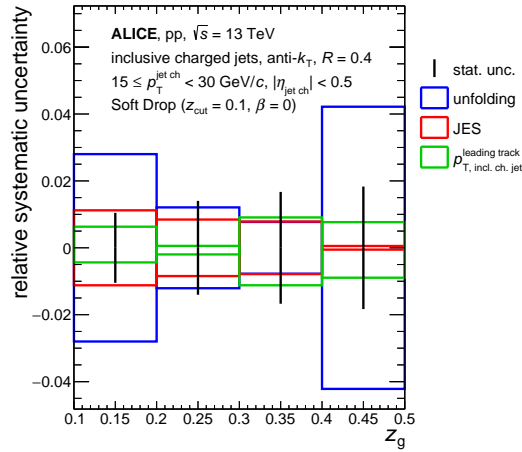


Figure A.7: The systematic uncertainties of the measured z_g distribution of inclusive jets for each uncertainty category, relative to the central value of the measurement in each interval, are presented. The statistical uncertainty relative to the central value is also shown.

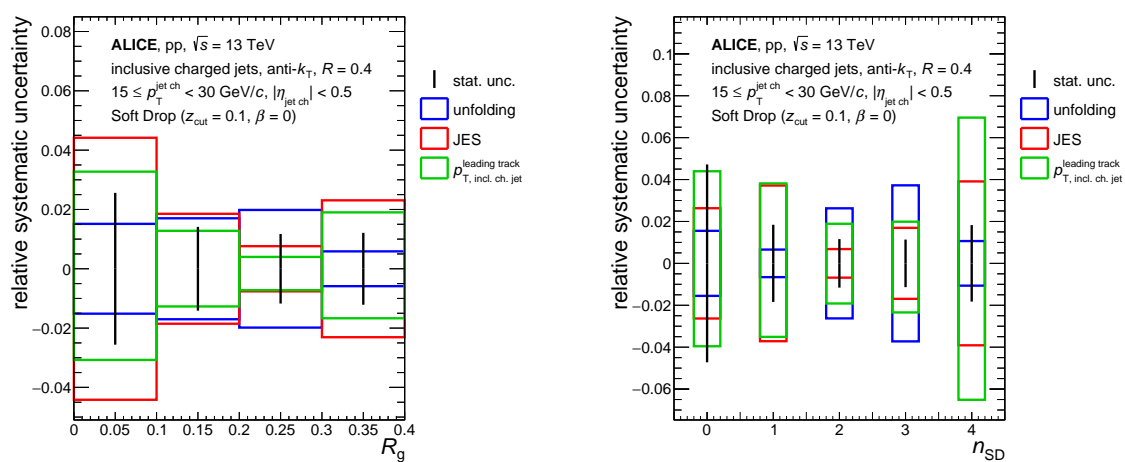











Figure A.8: The systematic uncertainties of the measured R_g (left) and n_{SD} (right) distributions of inclusive jets for each uncertainty category, relative to the central value of the measurement in each interval, are presented. The statistical uncertainty relative to the central value is also shown.

B The ALICE Collaboration

S. Acharya ¹²⁵, D. Adamová ⁸⁶, A. Adler⁶⁹, G. Aglieri Rinella ³², M. Agnello ²⁹, N. Agrawal ⁵⁰, Z. Ahammed ¹³², S. Ahmad ¹⁵, S.U. Ahn ⁷⁰, I. Ahuja ³⁷, A. Akindinov ¹⁴⁰, M. Al-Turany ⁹⁸, D. Aleksandrov ¹⁴⁰, B. Alessandro ⁵⁵, H.M. Alfanda ⁶, R. Alfaro Molina ⁶⁶, B. Ali ¹⁵, Y. Ali¹³, A. Alici ²⁵, N. Alizadehvandchali ¹¹⁴, A. Alkin ³², J. Alme ²⁰, G. Alocco ⁵¹, T. Alt ⁶³, I. Altsybeev ¹⁴⁰, M.N. Anaam ⁶, C. Andrei ⁴⁵, A. Andronic ¹³⁵, V. Anguelov ⁹⁵, F. Antinori ⁵³, P. Antonioli ⁵⁰, C. Anuj ¹⁵, N. Apadula ⁷⁴, L. Aphecetche ¹⁰⁴, H. Appelshäuser ⁶³, C. Arata ⁷³, S. Arcelli ²⁵, M. Aresti ⁵¹, R. Arnaldi ⁵⁵, I.C. Arsene ¹⁹, M. Arslandok ¹³⁷, A. Augustinus ³², R. Averbeck ⁹⁸, M.D. Azmi ¹⁵, A. Badalà ⁵², Y.W. Baek ⁴⁰, X. Bai ¹¹⁸, R. Bailhache ⁶³, Y. Bailung ⁴⁷, R. Bala ⁹¹, A. Balbino ²⁹, A. Baldisseri ¹²⁸, B. Balis ², D. Banerjee ⁴, Z. Banoo ⁹¹, R. Barbera ²⁶, F. Barile ³¹, L. Barioglio ⁹⁶, M. Barlou⁷⁸, G.G. Barnaföldi ¹³⁶, L.S. Barnby ⁸⁵, V. Barret ¹²⁵, L. Barreto ¹¹⁰, C. Bartels ¹¹⁷, K. Barth ³², E. Bartsch ⁶³, F. Baruffaldi ²⁷, N. Bastid ¹²⁵, S. Basu ⁷⁵, G. Batigne ¹⁰⁴, D. Battistini ⁹⁶, B. Batyunya ¹⁴¹, D. Bauri⁴⁶, J.L. Bazo Alba ¹⁰², I.G. Bearden ⁸³, C. Beattie ¹³⁷, P. Becht ⁹⁸, D. Behera ⁴⁷, I. Belikov ¹²⁷, A.D.C. Bell Hechavarria ¹³⁵, F. Bellini ²⁵, R. Bellwied ¹¹⁴, S. Belokurova ¹⁴⁰, V. Belyaev ¹⁴⁰, G. Bencedi ^{136,64}, S. Beole ²⁴, A. Bercuci ⁴⁵, Y. Berdnikov ¹⁴⁰, A. Berdnikova ⁹⁵, L. Bergmann ⁹⁵, M.G. Besoiu ⁶², L. Betev ³², P.P. Bhaduri ¹³², A. Bhasin ⁹¹, M.A. Bhat ⁴, B. Bhattacharjee ⁴¹, L. Bianchi ²⁴, N. Bianchi ⁴⁸, J. Bielčík ³⁵, J. Bielčíková ⁸⁶, J. Biernat ¹⁰⁷, A.P. Bigot ¹²⁷, A. Bilandzic ⁹⁶, G. Biro ¹³⁶, S. Biswas ⁴, N. Bize ¹⁰⁴, J.T. Blair ¹⁰⁸, D. Blau ¹⁴⁰, M.B. Blidaru ⁹⁸, N. Bluhme³⁸, C. Blume ⁶³, G. Boca ^{21,54}, F. Bock ⁸⁷, T. Bodova ²⁰, A. Bogdanov¹⁴⁰, S. Boi ²², J. Bok ⁵⁷, L. Boldizsár ¹³⁶, A. Bolozdynya ¹⁴⁰, M. Bombara ³⁷, P.M. Bond ³², G. Bonomi ^{131,54}, H. Borel ¹²⁸, A. Borissov ¹⁴⁰, H. Bossi ¹³⁷, E. Botta ²⁴, Y.E.M. Bouziani ⁶³, L. Bratrud ⁶³, P. Braun-Munzinger ⁹⁸, M. Bregant ¹¹⁰, M. Broz ³⁵, G.E. Bruno ^{97,31}, M.D. Buckland ¹¹⁷, D. Budnikov ¹⁴⁰, H. Buesching ⁶³, S. Bufalino ²⁹, O. Bugnon¹⁰⁴, P. Buhler ¹⁰³, Z. Buthelezi ^{67,121}, J.B. Butt¹³, S.A. Bysiak¹⁰⁷, M. Cai ⁶, H. Caines ¹³⁷, A. Caliva ⁹⁸, E. Calvo Villar ¹⁰², J.M.M. Camacho ¹⁰⁹, P. Camerini ²³, F.D.M. Canedo ¹¹⁰, M. Carabas ¹²⁴, F. Carnesecchi ³², R. Caron ¹²⁶, J. Castillo Castellanos ¹²⁸, F. Catalano ^{24,29}, C. Ceballos Sanchez ¹⁴¹, I. Chakaberia ⁷⁴, P. Chakraborty ⁴⁶, S. Chandra ¹³², S. Chapeland ³², M. Chartier ¹¹⁷, S. Chattopadhyay ¹³², S. Chattopadhyay ¹⁰⁰, T.G. Chavez ⁴⁴, T. Cheng ⁶, C. Cheshkov ¹²⁶, B. Cheynis ¹²⁶, V. Chibante Barroso ³², D.D. Chinellato ¹¹¹, E.S. Chizzali ^{11,96}, J. Cho ⁵⁷, S. Cho ⁵⁷, P. Chochula ³², P. Christakoglou ⁸⁴, C.H. Christensen ⁸³, P. Christiansen ⁷⁵, T. Chujo ¹²³, M. Ciaccio ²⁹, C. Cicalo ⁵¹, L. Cifarelli ²⁵, F. Cindolo ⁵⁰, M.R. Ciupek⁹⁸, G. Clai^{III,50}, F. Colamaria ⁴⁹, J.S. Colburn¹⁰¹, D. Colella ^{97,31}, M. Colocci ³², M. Concas ^{IV,55}, G. Conesa Balbastre ⁷³, Z. Conesa del Valle ⁷², G. Contin ²³, J.G. Contreras ³⁵, M.L. Coquet ¹²⁸, T.M. Cormier^{I,87}, P. Cortese ^{130,55}, M.R. Cosentino ¹¹², F. Costa ³², S. Costanza ^{21,54}, J. Crkovská ⁹⁵, P. Crochet ¹²⁵, R. Cruz-Torres ⁷⁴, E. Cuautle⁶⁴, P. Cui ⁶, L. Cunqueiro⁸⁷, A. Dainese ⁵³, M.C. Danisch ⁹⁵, A. Danu ⁶², P. Das ⁸⁰, P. Das ⁴, S. Das ⁴, A.R. Dash ¹³⁵, S. Dash ⁴⁶, R.M.H. David⁴⁴, A. De Caro ²⁸, G. de Cataldo ⁴⁹, J. de Cuveland³⁸, A. De Falco ²², D. De Gruttola ²⁸, N. De Marco ⁵⁵, C. De Martin ²³, S. De Pasquale ²⁸, S. Deb ⁴⁷, R.J. Debbski ², K.R. Deja¹³³, R. Del Grande ⁹⁶, L. Dello Stritto ²⁸, W. Deng ⁶, P. Dhankher ¹⁸, D. Di Bari ³¹, A. Di Mauro ³², R.A. Diaz ^{141,7}, T. Dietel ¹¹³, Y. Ding ^{126,6}, R. Divià ³², D.U. Dixit ¹⁸, Ø. Djuvsland²⁰, U. Dmitrieva ¹⁴⁰, A. Dobrin ⁶², B. Dönigus ⁶³, A.K. Dubey ¹³², J.M. Dubinski ¹³³, A. Dubla ⁹⁸, S. Dudi ⁹⁰, P. Dupieux ¹²⁵, M. Durkac¹⁰⁶, N. Dzalaiova¹², T.M. Eder ¹³⁵, R.J. Ehlers ⁸⁷, V.N. Eikeland²⁰, F. Eisenhut ⁶³, D. Elia ⁴⁹, B. Erazmus ¹⁰⁴, F. Ercolessi ²⁵, F. Erhardt ⁸⁹, M.R. Ersdal²⁰, B. Espagnon ⁷², G. Eulisse ³², D. Evans ¹⁰¹, S. Evdokimov ¹⁴⁰, L. Fabbietti ⁹⁶, M. Faggin ²⁷, J. Faivre ⁷³, F. Fan ⁶, W. Fan ⁷⁴, A. Fantoni ⁴⁸, M. Fasel ⁸⁷, P. Fedichio²⁹, A. Feliciello ⁵⁵, G. Feofilov ¹⁴⁰, A. Fernández Téllez ⁴⁴, M.B. Ferrer ³², A. Ferrero ¹²⁸, C. Ferrero ⁵⁵, A. Ferretti ²⁴, V.J.G. Feuillard ⁹⁵, V. Filova ³⁵, D. Finogeev ¹⁴⁰, F.M. Fionda ⁵¹, F. Flor ¹¹⁴, A.N. Flores ¹⁰⁸, S. Foertsch ⁶⁷, I. Fokin ⁹⁵, S. Fokin ¹⁴⁰, E. Fragiocomo ⁵⁶, E. Frajna ¹³⁶, U. Fuchs ³², N. Funicello ²⁸, C. Furget ⁷³, A. Furs ¹⁴⁰, T. Fusayasu ⁹⁹, J.J. Gaardhøje ⁸³, M. Gagliardi ²⁴, A.M. Gago ¹⁰², C.D. Galvan ¹⁰⁹, D.R. Gangadharan ¹¹⁴, P. Ganoti ⁷⁸, C. Garabatos ⁹⁸, J.R.A. Garcia ⁴⁴, E. Garcia-Solis ⁹, K. Garg ¹⁰⁴, C. Gargiulo ³², A. Garibli⁸¹, K. Garner¹³⁵, A. Gautam ¹¹⁶, M.B. Gay Ducati ⁶⁵, M. Germain ¹⁰⁴, C. Ghosh¹³², S.K. Ghosh⁴, M. Giacalone ²⁵, P. Gianotti ⁴⁸, P. Giubellino ^{98,55}, P. Giubilato ²⁷, A.M.C. Glaenzler ¹²⁸, P. Glässel ⁹⁵, E. Glimos ¹²⁰, D.J.Q. Goh⁷⁶, V. Gonzalez ¹³⁴, L.H. González-Trueba ⁶⁶, M. Gorgon ², S. Gotovac³³, V. Grabski ⁶⁶, L.K. Graczykowski ¹³³, E. Grecka ⁸⁶, A. Grelli ⁵⁸, C. Grigoras ³², V. Grigoriev ¹⁴⁰, S. Grigoryan ^{141,1}, F. Grosa ³², J.F. Grosse-Oetringhaus ³², R. Grosso ⁹⁸, D. Grund ³⁵, G.G. Guardiano ¹¹¹, R. Guernane ⁷³, M. Guilbaud ¹⁰⁴, K. Gulbrandsen ⁸³, T. Gundem ⁶³, T. Gunji ¹²², W. Guo ⁶,

A. Gupta ⁹¹, R. Gupta ⁹¹, S.P. Guzman ⁴⁴, L. Gyulai ¹³⁶, M.K. Habib ⁹⁸, C. Hadjidakis ⁷²,
 H. Hamagaki ⁷⁶, M. Hamid ⁶, Y. Han ¹³⁸, R. Hannigan ¹⁰⁸, M.R. Haque ¹³³, J.W. Harris ¹³⁷,
 A. Harton ⁹, H. Hassan ⁸⁷, D. Hatzifotiadou ⁵⁰, P. Hauer ⁴², L.B. Havener ¹³⁷, S.T. Heckel ⁹⁶,
 E. Hellbär ⁹⁸, H. Helstrup ³⁴, M. Hemmer ⁶³, T. Herman ³⁵, G. Herrera Corral ⁸, F. Herrmann ¹³⁵,
 S. Herrmann ¹²⁶, K.F. Hetland ³⁴, B. Heybeck ⁶³, H. Hillemanns ³², C. Hills ¹¹⁷, B. Hippolyte ¹²⁷,
 B. Hofman ⁵⁸, B. Hohlweger ⁸⁴, J. Honermann ¹³⁵, G.H. Hong ¹³⁸, A. Horzyk ², R. Hosokawa ¹⁴,
 Y. Hou ⁶, P. Hristov ³², C. Hughes ¹²⁰, P. Huhn ⁶³, L.M. Huhta ¹¹⁵, C.V. Hulse ⁷², T.J. Humanic ⁸⁸,
 H. Hushnud ¹⁰⁰, A. Hutson ¹¹⁴, D. Hutter ³⁸, J.P. Iddon ¹¹⁷, R. Ilkaev ¹⁴⁰, H. Ilyas ¹³, M. Inaba ¹²³,
 G.M. Innocenti ³², M. Ippolitov ¹⁴⁰, A. Isakov ⁸⁶, T. Isidori ¹¹⁶, M.S. Islam ¹⁰⁰, M. Ivanov ¹²,
 M. Ivanov ⁹⁸, V. Ivanov ¹⁴⁰, V. Izucheev ¹⁴⁰, M. Jablonski ², B. Jacak ⁷⁴, N. Jacazio ³², P.M. Jacobs ⁷⁴,
 S. Jadlovská ¹⁰⁶, J. Jadlovsky ¹⁰⁶, S. Jaelani ⁸², L. Jaffe ³⁸, C. Jahnke ¹¹¹, M.J. Jakubowska ¹³³,
 M.A. Janik ¹³³, T. Janson ⁶⁹, M. Jercic ⁸⁹, O. Jevons ¹⁰¹, A.A.P. Jimenez ⁶⁴, F. Jonas ⁸⁷, P.G. Jones ¹⁰¹,
 J.M. Jowett ^{32,98}, J. Jung ⁶³, M. Jung ⁶³, A. Junique ³², A. Jusko ¹⁰¹, M.J. Kabus ^{32,133}, J. Kaewjai ¹⁰⁵,
 P. Kalinak ⁵⁹, A.S. Kalteyer ⁹⁸, A. Kalweit ³², V. Kaplin ¹⁴⁰, A. Karasu Uysal ⁷¹, D. Karatovic ⁸⁹,
 O. Karavichev ¹⁴⁰, T. Karavicheva ¹⁴⁰, P. Karczmarczyk ¹³³, E. Karpechev ¹⁴⁰, V. Kashyap ⁸⁰,
 U. Keschull ⁶⁹, R. Keidel ¹³⁹, D.L.D. Keijdener ⁵⁸, M. Keil ³², B. Ketzer ⁴², A.M. Khan ⁶, S. Khan ¹⁵,
 A. Khanzadeev ¹⁴⁰, Y. Kharlov ¹⁴⁰, A. Khatun ¹⁵, A. Khuntia ¹⁰⁷, B. Kileng ³⁴, B. Kim ¹⁶,
 C. Kim ¹⁶, D.J. Kim ¹¹⁵, E.J. Kim ⁶⁸, J. Kim ¹³⁸, J.S. Kim ⁴⁰, J. Kim ⁹⁵, J. Kim ⁶⁸, M. Kim ⁹⁵,
 S. Kim ¹⁷, T. Kim ¹³⁸, K. Kimura ⁹³, S. Kirsch ⁶³, I. Kisel ³⁸, S. Kiselev ¹⁴⁰, A. Kisiel ¹³³,
 J.P. Kitowski ², J.L. Klay ⁵, J. Klein ³², S. Klein ⁷⁴, C. Klein-Bösing ¹³⁵, M. Kleiner ⁶³,
 T. Klemenz ⁹⁶, A. Kluge ³², A.G. Knospe ¹¹⁴, C. Kobdaj ¹⁰⁵, T. Kollegger ⁹⁸, A. Kondratyev ¹⁴¹,
 E. Kondratyuk ¹⁴⁰, J. Konig ⁶³, S.A. Konigstorfer ⁹⁶, P.J. Konopka ³², G. Kornakov ¹³³,
 S.D. Koryciak ², A. Kotliarov ⁸⁶, O. Kovalenko ⁷⁹, V. Kovalenko ¹⁴⁰, M. Kowalski ¹⁰⁷, I. Králik ⁵⁹,
 A. Kravčáková ³⁷, L. Kreis ⁹⁸, M. Krivda ^{101,59}, F. Krizek ⁸⁶, K. Krizkova Gajdosova ³⁵, M. Kroesen ⁹⁵,
 M. Krüger ⁶³, D.M. Krupova ³⁵, E. Kryshen ¹⁴⁰, V. Kučera ³², C. Kuhn ¹²⁷, P.G. Kuijjer ⁸⁴,
 T. Kumaoka ¹²³, D. Kumar ¹³², L. Kumar ⁹⁰, N. Kumar ⁹⁰, S. Kumar ³¹, S. Kundu ³², P. Kurashvili ⁷⁹,
 A. Kurepin ¹⁴⁰, A.B. Kurepin ¹⁴⁰, S. Kushpil ⁸⁶, J. Kvapil ¹⁰¹, M.J. Kweon ⁵⁷, J.Y. Kwon ⁵⁷,
 Y. Kwon ¹³⁸, S.L. La Pointe ³⁸, P. La Rocca ²⁶, Y.S. Lai ⁷⁴, A. Lakrathok ¹⁰⁵, M. Lamanna ³²,
 R. Langoy ¹¹⁹, P. Larionov ³², E. Laudi ³², L. Lautner ^{32,96}, R. Lavicka ¹⁰³, T. Lazareva ¹⁴⁰,
 R. Lea ^{131,54}, G. Legras ¹³⁵, J. Lehrbach ³⁸, R.C. Lemmon ⁸⁵, I. León Monzón ¹⁰⁹, M.M. Lesch ⁹⁶,
 E.D. Lesser ¹⁸, M. Lettrich ⁹⁶, P. Lévai ¹³⁶, X. Li ¹⁰, X.L. Li ⁶, J. Lien ¹¹⁹, R. Lietava ¹⁰¹, B. Lim ¹⁶,
 S.H. Lim ¹⁶, V. Lindenstruth ³⁸, A. Lindner ⁴⁵, C. Lippmann ⁹⁸, A. Liu ¹⁸, D.H. Liu ⁶, J. Liu ¹¹⁷,
 I.M. Lofnes ²⁰, C. Loizides ⁸⁷, P. Loncar ³³, J.A. Lopez ⁹⁵, X. Lopez ¹²⁵, E. López Torres ⁷,
 P. Lu ^{98,118}, J.R. Luhder ¹³⁵, M. Lunardon ²⁷, G. Luparello ⁵⁶, Y.G. Ma ³⁹, A. Maevskaya ¹⁴⁰,
 M. Mager ³², T. Mahmoud ⁴², A. Maire ¹²⁷, M. Malaev ¹⁴⁰, G. Malfattore ²⁵, N.M. Malik ⁹¹,
 Q.W. Malik ¹⁹, S.K. Malik ⁹¹, L. Malinina ^{VII,141}, D. Mal'Kevich ¹⁴⁰, D. Mallick ⁸⁰, N. Mallick ⁴⁷,
 G. Mandaglio ^{30,52}, V. Manko ¹⁴⁰, F. Manso ¹²⁵, V. Manzari ⁴⁹, Y. Mao ⁶, G.V. Margagliotti ²³,
 A. Margotti ⁵⁰, A. Marín ⁹⁸, C. Markert ¹⁰⁸, P. Martinengo ³², J.L. Martínez ¹¹⁴, M.I. Martínez ⁴⁴,
 G. Martínez García ¹⁰⁴, S. Masciocchi ⁹⁸, M. Maserà ²⁴, A. Masoni ⁵¹, L. Massacrier ⁷²,
 A. Mastroserio ^{129,49}, A.M. Mathis ⁹⁶, O. Matonoha ⁷⁵, P.F.T. Matuoka ¹¹⁰, A. Matyja ¹⁰⁷, C. Mayer ¹⁰⁷,
 A.L. Mazuecos ³², F. Mazzaschi ²⁴, M. Mazzilli ³², J.E. Mdhuli ¹²¹, A.F. Mechler ⁶³, Y. Melikyan ¹⁴⁰,
 A. Menchaca-Rocha ⁶⁶, E. Meninno ^{103,28}, A.S. Menon ¹¹⁴, M. Meres ¹², S. Mhlanga ^{113,67}, Y. Miake ¹²³,
 L. Micheletti ⁵⁵, L.C. Migliorin ¹²⁶, D.L. Mihaylov ⁹⁶, K. Mikhaylov ^{141,140}, A.N. Mishra ¹³⁶,
 D. Miśkowiec ⁹⁸, A. Modak ⁴, A.P. Mohanty ⁵⁸, B. Mohanty ⁸⁰, M. Mohisin Khan ^{V,15},
 M.A. Molander ⁴³, Z. Moravcova ⁸³, C. Mordasini ⁹⁶, D.A. Moreira De Godoy ¹³⁵, I. Morozov ¹⁴⁰,
 A. Morsch ³², T. Mrnjavac ³², V. Muccifora ⁴⁸, S. Muhuri ¹³², J.D. Mulligan ⁷⁴, A. Mulliri ²²,
 M.G. Munhoz ¹¹⁰, R.H. Munzer ⁶³, H. Murakami ¹²², S. Murray ¹¹³, L. Musa ³², J. Musinsky ⁵⁹,
 J.W. Myrcha ¹³³, B. Naik ¹²¹, R. Nair ⁷⁹, A.I. Nambrath ¹⁸, B.K. Nandi ⁴⁶, R. Nania ⁵⁰, E. Nappi ⁴⁹,
 A.F. Nassirpour ⁷⁵, A. Nath ⁹⁵, C. Nattrass ¹²⁰, A. Neagu ¹⁹, A. Negru ¹²⁴, L. Nellen ⁶⁴, S.V. Nesbo ³⁴,
 G. Neskovic ³⁸, D. Nesterov ¹⁴⁰, B.S. Nielsen ⁸³, E.G. Nielsen ⁸³, S. Nikolaev ¹⁴⁰, S. Nikulin ¹⁴⁰,
 V. Nikulin ¹⁴⁰, F. Noferini ⁵⁰, S. Noh ¹¹, P. Nomokonov ¹⁴¹, J. Norman ¹¹⁷, N. Novitzky ¹²³,
 P. Nowakowski ¹³³, A. Nyanin ¹⁴⁰, J. Nystrand ²⁰, M. Ogino ⁷⁶, A. Ohlson ⁷⁵, V.A. Okorokov ¹⁴⁰,
 J. Olińczak ¹³³, A.C. Oliveira Da Silva ¹²⁰, M.H. Oliver ¹³⁷, A. Onnerstad ¹¹⁵, C. Oppedisano ⁵⁵,
 A. Ortiz Velasquez ⁶⁴, A. Oskarsson ⁷⁵, J. Otwinowski ¹⁰⁷, M. Oya ⁹³, K. Oyama ⁷⁶, Y. Pachmayer ⁹⁵,
 S. Padhan ⁴⁶, D. Pagano ^{131,54}, G. Paic ⁶⁴, A. Palasciano ⁴⁹, S. Panebianco ¹²⁸, H. Park ¹²³,
 J. Park ⁵⁷, J.E. Parkkila ³², R.N. Patra ⁹¹, B. Paul ²², H. Pei ⁶, T. Peitzmann ⁵⁸, X. Peng ⁶,

M. Pennisi ²⁴, L.G. Pereira ⁶⁵, H. Pereira Da Costa ¹²⁸, D. Peresunko ¹⁴⁰, G.M. Perez ⁷, S. Perrin ¹²⁸,
 Y. Pestov ¹⁴⁰, V. Petráček ³⁵, V. Petrov ¹⁴⁰, M. Petrovici ⁴⁵, R.P. Pezzi ^{104,65}, S. Piano ⁵⁶, M. Pikna ¹²,
 P. Pillot ¹⁰⁴, O. Pinazza ^{50,32}, L. Pinsky ¹¹⁴, C. Pinto ⁹⁶, S. Pisano ⁴⁸, M. Płoskoń ⁷⁴, M. Planinic ⁸⁹,
 F. Pliquet ⁶³, M.G. Poghosyan ⁸⁷, S. Politano ²⁹, N. Poljak ⁸⁹, A. Pop ⁴⁵, S. Porteboeuf-Houssais ¹²⁵,
 J. Porter ⁷⁴, V. Pozdniakov ¹⁴¹, S.K. Prasad ⁴, S. Prasad ⁴⁷, R. Preghenella ⁵⁰, F. Prino ⁵⁵,
 C.A. Pruneau ¹³⁴, I. Pshenichnov ¹⁴⁰, M. Puccio ³², S. Pucillo ²⁴, Z. Pugelova ¹⁰⁶, S. Qiu ⁸⁴,
 L. Quaglia ²⁴, R.E. Quishpe ¹¹⁴, S. Ragoni ^{14,101}, A. Rakotozafindrabe ¹²⁸, L. Ramello ^{130,55},
 F. Rami ¹²⁷, S.A.R. Ramirez ⁴⁴, T.A. Rancien ⁷³, R. Raniwala ⁹², S. Raniwala ⁹², M. Rasa ²⁶,
 S.S. Räsänen ⁴³, R. Rath ^{50,47}, I. Ravasenga ⁸⁴, K.F. Read ^{87,120}, C. Reckziegel ¹¹², A.R. Redelbach ³⁸,
 K. Redlich ^{VI,79}, A. Rehman ²⁰, F. Reidt ³², H.A. Reme-Ness ³⁴, Z. Rescakova ³⁷, K. Reygers ⁹⁵,
 A. Riabov ¹⁴⁰, V. Riabov ¹⁴⁰, R. Ricci ²⁸, T. Richert ⁷⁵, M. Richter ¹⁹, A.A. Riedel ⁹⁶, W. Riegler ³²,
 F. Riggi ²⁶, C. Ristea ⁶², M. Rodríguez Cahuantzi ⁴⁴, K. Røed ¹⁹, R. Rogalev ¹⁴⁰, E. Rogochaya ¹⁴¹,
 T.S. Rogoschinski ⁶³, D. Rohr ³², D. Röhrich ²⁰, P.F. Rojas ⁴⁴, S. Rojas Torres ³⁵, P.S. Rokita ¹³³,
 G. Romanenko ¹⁴¹, F. Ronchetti ⁴⁸, A. Rosano ^{30,52}, E.D. Rosas ⁶⁴, A. Rossi ⁵³, A. Roy ⁴⁷, P. Roy ¹⁰⁰,
 S. Roy ⁴⁶, N. Rubini ²⁵, O.V. Rueda ⁷⁵, D. Ruggiano ¹³³, R. Rui ²³, B. Rumyantsev ¹⁴¹, P.G. Russek ²,
 R. Russo ⁸⁴, A. Rustamov ⁸¹, E. Ryabinkin ¹⁴⁰, Y. Ryabov ¹⁴⁰, A. Rybicki ¹⁰⁷, H. Rytönen ¹¹⁵,
 W. Rzesza ¹³³, O.A.M. Saarimäki ⁴³, R. Sadek ¹⁰⁴, S. Sadhu ³¹, S. Sadovsky ¹⁴⁰, J. Saetre ²⁰,
 K. Šafařík ³⁵, S.K. Saha ⁴, S. Saha ⁸⁰, B. Sahoo ⁴⁶, R. Sahoo ⁴⁷, S. Sahoo ⁶⁰, D. Sahu ⁴⁷,
 P.K. Sahu ⁶⁰, J. Saini ¹³², K. Sajdakova ³⁷, S. Sakai ¹²³, M.P. Salvan ⁹⁸, S. Sambyal ⁹¹, T.B. Saramela ¹¹⁰,
 D. Sarkar ¹³⁴, N. Sarkar ¹³², P. Sarma ⁴¹, V. Sarritzu ²², V.M. Sarti ⁹⁶, M.H.P. Sas ¹³⁷, J. Schambach ⁸⁷,
 H.S. Scheid ⁶³, C. Schiaua ⁴⁵, R. Schicker ⁹⁵, A. Schmah ⁹⁵, C. Schmidt ⁹⁸, H.R. Schmidt ⁹⁴,
 M.O. Schmidt ³², M. Schmidt ⁹⁴, N.V. Schmidt ⁸⁷, A.R. Schmier ¹²⁰, R. Schotter ¹²⁷, J. Schukraft ³²,
 K. Schwarz ⁹⁸, K. Schweda ⁹⁸, G. Scioli ²⁵, E. Scomparin ⁵⁵, J.E. Seger ¹⁴, Y. Sekiguchi ¹²²,
 D. Sekihata ¹²², I. Selyuzhenkov ^{98,140}, S. Senyukov ¹²⁷, J.J. Seo ⁵⁷, D. Serebryakov ¹⁴⁰,
 L. Šerkšnytė ⁹⁶, A. Sevcenco ⁶², T.J. Shaba ⁶⁷, A. Shabetai ¹⁰⁴, R. Shahoyan ³², A. Shangaraev ¹⁴⁰,
 A. Sharma ⁹⁰, D. Sharma ⁴⁶, H. Sharma ¹⁰⁷, M. Sharma ⁹¹, N. Sharma ⁹⁰, S. Sharma ⁷⁶, S. Sharma ⁹¹,
 U. Sharma ⁹¹, A. Shatat ⁷², O. Sheibani ¹¹⁴, K. Shigaki ⁹³, M. Shimomura ⁷⁷, S. Shirinkin ¹⁴⁰, Q. Shou ³⁹,
 Y. Sibiriak ¹⁴⁰, S. Siddhanta ⁵¹, T. Siemiarczuk ⁷⁹, T.F. Silva ¹¹⁰, D. Silvermyr ⁷⁵,
 T. Simantathammakul ¹⁰⁵, R. Simeonov ³⁶, B. Singh ⁹¹, B. Singh ⁹⁶, R. Singh ⁸⁰, R. Singh ⁹¹, R. Singh ⁴⁷,
 S. Singh ¹⁵, V.K. Singh ¹³², V. Singhal ¹³², T. Sinha ¹⁰⁰, B. Sitar ¹², M. Sitta ^{130,55}, T.B. Skaali ¹⁹,
 G. Skorodumovs ⁹⁵, M. Slupecki ⁴³, N. Smirnov ¹³⁷, R.J.M. Snellings ⁵⁸, E.H. Solheim ¹⁹, J. Song ¹¹⁴,
 A. Songmoolnak ¹⁰⁵, F. Soramel ²⁷, S. Sorensen ¹²⁰, R. Spijkers ⁸⁴, I. Sputowska ¹⁰⁷, J. Staa ⁷⁵,
 J. Stachel ⁹⁵, I. Stan ⁶², P.J. Steffanic ¹²⁰, S.F. Stiefelmaier ⁹⁵, D. Stocco ¹⁰⁴, I. Storehaug ¹⁹,
 M.M. Støretvedt ³⁴, P. Stratmann ¹³⁵, S. Strazzi ²⁵, C.P. Stylianidis ⁸⁴, A.A.P. Suaide ¹¹⁰, C. Suire ⁷²,
 M. Sukhanov ¹⁴⁰, M. Suljic ³², V. Sumberia ⁹¹, S. Sumowidagdo ⁸², S. Swain ⁶⁰, I. Szarka ¹²,
 U. Tabassam ¹³, S.F. Taghavi ⁹⁶, G. Taillepiéd ⁹⁸, J. Takahashi ¹¹¹, G.J. Tambave ²⁰, S. Tang ^{125,6},
 Z. Tang ¹¹⁸, J.D. Tapia Takaki ¹¹⁶, N. Tapus ¹²⁴, L.A. Tarasovicova ¹³⁵, M.G. Tazila ⁴⁵, G.F. Tassielli ³¹,
 A. Tauro ³², A. Telesca ³², L. Terlizzi ²⁴, C. Terrevoli ¹¹⁴, G. Tersimonov ³, S. Thakur ⁴, D. Thomas ¹⁰⁸,
 A. Tikhonov ¹⁴⁰, A.R. Timmins ¹¹⁴, M. Tkacik ¹⁰⁶, T. Tkacik ¹⁰⁶, A. Toia ⁶³, R. Tokumoto ⁹³,
 N. Topilskaya ¹⁴⁰, M. Toppi ⁴⁸, F. Torales-Acosta ¹⁸, T. Tork ⁷², A.G. Torres Ramos ³¹, A. Trifiró ^{30,52},
 A.S. Triolo ^{30,52}, S. Tripathy ⁵⁰, T. Tripathy ⁴⁶, S. Trogolo ³², V. Trubnikov ³, W.H. Trzaska ¹¹⁵,
 T.P. Trzcinski ¹³³, R. Turrisi ⁵³, T.S. Tveter ¹⁹, K. Ullaland ²⁰, B. Ulukutlu ⁹⁶, A. Uras ¹²⁶,
 M. Urioni ^{54,131}, G.L. Usai ²², M. Vala ³⁷, N. Valle ²¹, S. Vallero ⁵⁵, L.V.R. van Doremalen ⁵⁸, M. van
 Leeuwen ⁸⁴, C.A. van Veen ⁹⁵, R.J.G. van Weelden ⁸⁴, P. Vande Vyvre ³², D. Varga ¹³⁶, Z. Varga ¹³⁶,
 M. Varga-Kofarago ¹³⁶, M. Vasileiou ⁷⁸, A. Vasiliev ¹⁴⁰, O. Vázquez Doce ⁴⁸, V. Vechernin ¹⁴⁰,
 E. Vercellin ²⁴, S. Vergara Limón ⁴⁴, L. Vermunt ⁹⁸, R. Vértesi ¹³⁶, M. Verweij ⁵⁸, L. Vickovic ³³,
 Z. Vilakazi ¹²¹, O. Villalobos Baillie ¹⁰¹, G. Vino ⁴⁹, A. Vinogradov ¹⁴⁰, T. Virgili ²⁸, V. Vislavicius ⁸³,
 A. Vodopyanov ¹⁴¹, B. Volkel ³², M.A. Völkl ⁹⁵, K. Voloshin ¹⁴⁰, S.A. Voloshin ¹³⁴, G. Volpe ³¹, B. von
 Haller ³², I. Vorobyev ⁹⁶, N. Vozniuk ¹⁴⁰, J. Vrláková ³⁷, B. Wagner ²⁰, C. Wang ³⁹, D. Wang ³⁹,
 A. Wegrzynek ³², F.T. Weiglhofer ³⁸, S.C. Wenzel ³², J.P. Wessels ¹³⁵, S.L. Weyhmler ¹³⁷,
 J. Wiechula ⁶³, J. Wikne ¹⁹, G. Wilk ⁷⁹, J. Wilkinson ⁹⁸, G.A. Willems ¹³⁵, B. Windelband ⁹⁵,
 M. Winn ¹²⁸, J.R. Wright ¹⁰⁸, W. Wu ³⁹, Y. Wu ¹¹⁸, R. Xu ⁶, A. Yadav ⁴², A.K. Yadav ¹³²,
 S. Yalcin ⁷¹, Y. Yamaguchi ⁹³, K. Yamakawa ⁹³, S. Yang ²⁰, S. Yano ⁹³, Z. Yin ⁶, I.-K. Yoo ¹⁶,
 J.H. Yoon ⁵⁷, S. Yuan ²⁰, A. Yuncu ⁹⁵, V. Zaccolo ²³, C. Zampolli ³², H.J.C. Zanoli ⁵⁸, F. Zanone ⁹⁵,
 N. Zardoshti ^{32,101}, A. Zarochentsev ¹⁴⁰, P. Závada ⁶¹, N. Zaviyalov ¹⁴⁰, M. Zhalov ¹⁴⁰, B. Zhang ⁶,

S. Zhang ³⁹, X. Zhang ⁶, Y. Zhang¹¹⁸, Z. Zhang ⁶, M. Zhao ¹⁰, V. Zherebchevskii ¹⁴⁰, Y. Zhi¹⁰, N. Zhigareva¹⁴⁰, D. Zhou ⁶, Y. Zhou ⁸³, J. Zhu ^{98,6}, Y. Zhu⁶, G. Zinovjev^{1,3}, N. Zurlo ^{131,54}

Affiliation Notes

^I Deceased

^{II} Also at: Max-Planck-Institut für Physik, Munich, Germany

^{III} Also at: Italian National Agency for New Technologies, Energy and Sustainable Economic Development (ENEA), Bologna, Italy

^{IV} Also at: Dipartimento DET del Politecnico di Torino, Turin, Italy

^V Also at: Department of Applied Physics, Aligarh Muslim University, Aligarh, India

^{VI} Also at: Institute of Theoretical Physics, University of Wrocław, Poland

^{VII} Also at: An institution covered by a cooperation agreement with CERN

Collaboration Institutes

¹ A.I. Alikhanyan National Science Laboratory (Yerevan Physics Institute) Foundation, Yerevan, Armenia

² AGH University of Science and Technology, Cracow, Poland

³ Bogolyubov Institute for Theoretical Physics, National Academy of Sciences of Ukraine, Kiev, Ukraine

⁴ Bose Institute, Department of Physics and Centre for Astroparticle Physics and Space Science (CAPSS), Kolkata, India

⁵ California Polytechnic State University, San Luis Obispo, California, United States

⁶ Central China Normal University, Wuhan, China

⁷ Centro de Aplicaciones Tecnológicas y Desarrollo Nuclear (CEADEN), Havana, Cuba

⁸ Centro de Investigación y de Estudios Avanzados (CINVESTAV), Mexico City and Mérida, Mexico

⁹ Chicago State University, Chicago, Illinois, United States

¹⁰ China Institute of Atomic Energy, Beijing, China

¹¹ Chungbuk National University, Cheongju, Republic of Korea

¹² Comenius University Bratislava, Faculty of Mathematics, Physics and Informatics, Bratislava, Slovak Republic

¹³ COMSATS University Islamabad, Islamabad, Pakistan

¹⁴ Creighton University, Omaha, Nebraska, United States

¹⁵ Department of Physics, Aligarh Muslim University, Aligarh, India

¹⁶ Department of Physics, Pusan National University, Pusan, Republic of Korea

¹⁷ Department of Physics, Sejong University, Seoul, Republic of Korea

¹⁸ Department of Physics, University of California, Berkeley, California, United States

¹⁹ Department of Physics, University of Oslo, Oslo, Norway

²⁰ Department of Physics and Technology, University of Bergen, Bergen, Norway

²¹ Dipartimento di Fisica, Università di Pavia, Pavia, Italy

²² Dipartimento di Fisica dell'Università and Sezione INFN, Cagliari, Italy

²³ Dipartimento di Fisica dell'Università and Sezione INFN, Trieste, Italy

²⁴ Dipartimento di Fisica dell'Università and Sezione INFN, Turin, Italy

²⁵ Dipartimento di Fisica e Astronomia dell'Università and Sezione INFN, Bologna, Italy

²⁶ Dipartimento di Fisica e Astronomia dell'Università and Sezione INFN, Catania, Italy

²⁷ Dipartimento di Fisica e Astronomia dell'Università and Sezione INFN, Padova, Italy

²⁸ Dipartimento di Fisica 'E.R. Caianiello' dell'Università and Gruppo Collegato INFN, Salerno, Italy

²⁹ Dipartimento DISAT del Politecnico and Sezione INFN, Turin, Italy

³⁰ Dipartimento di Scienze MIFT, Università di Messina, Messina, Italy

³¹ Dipartimento Interateneo di Fisica 'M. Merlin' and Sezione INFN, Bari, Italy

³² European Organization for Nuclear Research (CERN), Geneva, Switzerland

³³ Faculty of Electrical Engineering, Mechanical Engineering and Naval Architecture, University of Split, Split, Croatia

³⁴ Faculty of Engineering and Science, Western Norway University of Applied Sciences, Bergen, Norway

³⁵ Faculty of Nuclear Sciences and Physical Engineering, Czech Technical University in Prague, Prague, Czech Republic

³⁶ Faculty of Physics, Sofia University, Sofia, Bulgaria

³⁷ Faculty of Science, P.J. Šafárik University, Košice, Slovak Republic

- ³⁸ Frankfurt Institute for Advanced Studies, Johann Wolfgang Goethe-Universität Frankfurt, Frankfurt, Germany
- ³⁹ Fudan University, Shanghai, China
- ⁴⁰ Gangneung-Wonju National University, Gangneung, Republic of Korea
- ⁴¹ Gauhati University, Department of Physics, Guwahati, India
- ⁴² Helmholtz-Institut für Strahlen- und Kernphysik, Rheinische Friedrich-Wilhelms-Universität Bonn, Bonn, Germany
- ⁴³ Helsinki Institute of Physics (HIP), Helsinki, Finland
- ⁴⁴ High Energy Physics Group, Universidad Autónoma de Puebla, Puebla, Mexico
- ⁴⁵ Horia Hulubei National Institute of Physics and Nuclear Engineering, Bucharest, Romania
- ⁴⁶ Indian Institute of Technology Bombay (IIT), Mumbai, India
- ⁴⁷ Indian Institute of Technology Indore, Indore, India
- ⁴⁸ INFN, Laboratori Nazionali di Frascati, Frascati, Italy
- ⁴⁹ INFN, Sezione di Bari, Bari, Italy
- ⁵⁰ INFN, Sezione di Bologna, Bologna, Italy
- ⁵¹ INFN, Sezione di Cagliari, Cagliari, Italy
- ⁵² INFN, Sezione di Catania, Catania, Italy
- ⁵³ INFN, Sezione di Padova, Padova, Italy
- ⁵⁴ INFN, Sezione di Pavia, Pavia, Italy
- ⁵⁵ INFN, Sezione di Torino, Turin, Italy
- ⁵⁶ INFN, Sezione di Trieste, Trieste, Italy
- ⁵⁷ Inha University, Incheon, Republic of Korea
- ⁵⁸ Institute for Gravitational and Subatomic Physics (GRASP), Utrecht University/Nikhef, Utrecht, Netherlands
- ⁵⁹ Institute of Experimental Physics, Slovak Academy of Sciences, Košice, Slovak Republic
- ⁶⁰ Institute of Physics, Homi Bhabha National Institute, Bhubaneswar, India
- ⁶¹ Institute of Physics of the Czech Academy of Sciences, Prague, Czech Republic
- ⁶² Institute of Space Science (ISS), Bucharest, Romania
- ⁶³ Institut für Kernphysik, Johann Wolfgang Goethe-Universität Frankfurt, Frankfurt, Germany
- ⁶⁴ Instituto de Ciencias Nucleares, Universidad Nacional Autónoma de México, Mexico City, Mexico
- ⁶⁵ Instituto de Física, Universidade Federal do Rio Grande do Sul (UFRGS), Porto Alegre, Brazil
- ⁶⁶ Instituto de Física, Universidad Nacional Autónoma de México, Mexico City, Mexico
- ⁶⁷ iThemba LABS, National Research Foundation, Somerset West, South Africa
- ⁶⁸ Jeonbuk National University, Jeonju, Republic of Korea
- ⁶⁹ Johann-Wolfgang-Goethe Universität Frankfurt Institut für Informatik, Fachbereich Informatik und Mathematik, Frankfurt, Germany
- ⁷⁰ Korea Institute of Science and Technology Information, Daejeon, Republic of Korea
- ⁷¹ KTO Karatay University, Konya, Turkey
- ⁷² Laboratoire de Physique des 2 Infinis, Irène Joliot-Curie, Orsay, France
- ⁷³ Laboratoire de Physique Subatomique et de Cosmologie, Université Grenoble-Alpes, CNRS-IN2P3, Grenoble, France
- ⁷⁴ Lawrence Berkeley National Laboratory, Berkeley, California, United States
- ⁷⁵ Lund University Department of Physics, Division of Particle Physics, Lund, Sweden
- ⁷⁶ Nagasaki Institute of Applied Science, Nagasaki, Japan
- ⁷⁷ Nara Women's University (NWU), Nara, Japan
- ⁷⁸ National and Kapodistrian University of Athens, School of Science, Department of Physics, Athens, Greece
- ⁷⁹ National Centre for Nuclear Research, Warsaw, Poland
- ⁸⁰ National Institute of Science Education and Research, Homi Bhabha National Institute, Jatni, India
- ⁸¹ National Nuclear Research Center, Baku, Azerbaijan
- ⁸² National Research and Innovation Agency - BRIN, Jakarta, Indonesia
- ⁸³ Niels Bohr Institute, University of Copenhagen, Copenhagen, Denmark
- ⁸⁴ Nikhef, National institute for subatomic physics, Amsterdam, Netherlands
- ⁸⁵ Nuclear Physics Group, STFC Daresbury Laboratory, Daresbury, United Kingdom
- ⁸⁶ Nuclear Physics Institute of the Czech Academy of Sciences, Husinec-Řež, Czech Republic
- ⁸⁷ Oak Ridge National Laboratory, Oak Ridge, Tennessee, United States
- ⁸⁸ Ohio State University, Columbus, Ohio, United States
- ⁸⁹ Physics department, Faculty of science, University of Zagreb, Zagreb, Croatia
- ⁹⁰ Physics Department, Panjab University, Chandigarh, India

- ⁹¹ Physics Department, University of Jammu, Jammu, India
⁹² Physics Department, University of Rajasthan, Jaipur, India
⁹³ Physics Program and International Institute for Sustainability with Knotted Chiral Meta Matter (SKCM2), Hiroshima University, Hiroshima, Japan
⁹⁴ Physikalisches Institut, Eberhard-Karls-Universität Tübingen, Tübingen, Germany
⁹⁵ Physikalisches Institut, Ruprecht-Karls-Universität Heidelberg, Heidelberg, Germany
⁹⁶ Physik Department, Technische Universität München, Munich, Germany
⁹⁷ Politecnico di Bari and Sezione INFN, Bari, Italy
⁹⁸ Research Division and ExtreMe Matter Institute EMMI, GSI Helmholtzzentrum für Schwerionenforschung GmbH, Darmstadt, Germany
⁹⁹ Saga University, Saga, Japan
¹⁰⁰ Saha Institute of Nuclear Physics, Homi Bhabha National Institute, Kolkata, India
¹⁰¹ School of Physics and Astronomy, University of Birmingham, Birmingham, United Kingdom
¹⁰² Sección Física, Departamento de Ciencias, Pontificia Universidad Católica del Perú, Lima, Peru
¹⁰³ Stefan Meyer Institut für Subatomare Physik (SMI), Vienna, Austria
¹⁰⁴ SUBATECH, IMT Atlantique, Nantes Université, CNRS-IN2P3, Nantes, France
¹⁰⁵ Suranaree University of Technology, Nakhon Ratchasima, Thailand
¹⁰⁶ Technical University of Košice, Košice, Slovak Republic
¹⁰⁷ The Henryk Niewodniczanski Institute of Nuclear Physics, Polish Academy of Sciences, Cracow, Poland
¹⁰⁸ The University of Texas at Austin, Austin, Texas, United States
¹⁰⁹ Universidad Autónoma de Sinaloa, Culiacán, Mexico
¹¹⁰ Universidade de São Paulo (USP), São Paulo, Brazil
¹¹¹ Universidade Estadual de Campinas (UNICAMP), Campinas, Brazil
¹¹² Universidade Federal do ABC, Santo Andre, Brazil
¹¹³ University of Cape Town, Cape Town, South Africa
¹¹⁴ University of Houston, Houston, Texas, United States
¹¹⁵ University of Jyväskylä, Jyväskylä, Finland
¹¹⁶ University of Kansas, Lawrence, Kansas, United States
¹¹⁷ University of Liverpool, Liverpool, United Kingdom
¹¹⁸ University of Science and Technology of China, Hefei, China
¹¹⁹ University of South-Eastern Norway, Kongsberg, Norway
¹²⁰ University of Tennessee, Knoxville, Tennessee, United States
¹²¹ University of the Witwatersrand, Johannesburg, South Africa
¹²² University of Tokyo, Tokyo, Japan
¹²³ University of Tsukuba, Tsukuba, Japan
¹²⁴ University Politehnica of Bucharest, Bucharest, Romania
¹²⁵ Université Clermont Auvergne, CNRS/IN2P3, LPC, Clermont-Ferrand, France
¹²⁶ Université de Lyon, CNRS/IN2P3, Institut de Physique des 2 Infinis de Lyon, Lyon, France
¹²⁷ Université de Strasbourg, CNRS, IPHC UMR 7178, F-67000 Strasbourg, France, Strasbourg, France
¹²⁸ Université Paris-Saclay Centre d'Etudes de Saclay (CEA), IRFU, Département de Physique Nucléaire (DPhN), Saclay, France
¹²⁹ Università degli Studi di Foggia, Foggia, Italy
¹³⁰ Università del Piemonte Orientale, Vercelli, Italy
¹³¹ Università di Brescia, Brescia, Italy
¹³² Variable Energy Cyclotron Centre, Homi Bhabha National Institute, Kolkata, India
¹³³ Warsaw University of Technology, Warsaw, Poland
¹³⁴ Wayne State University, Detroit, Michigan, United States
¹³⁵ Westfälische Wilhelms-Universität Münster, Institut für Kernphysik, Münster, Germany
¹³⁶ Wigner Research Centre for Physics, Budapest, Hungary
¹³⁷ Yale University, New Haven, Connecticut, United States
¹³⁸ Yonsei University, Seoul, Republic of Korea
¹³⁹ Zentrum für Technologie und Transfer (ZTT), Worms, Germany
¹⁴⁰ Affiliated with an institute covered by a cooperation agreement with CERN
¹⁴¹ Affiliated with an international laboratory covered by a cooperation agreement with CERN.